

Supporting Information

Ultrafast glutamate sensors resolve high-frequency release at Schaffer collateral synapses

Nordine Helassa^{a1*}, Céline D. Dürst^{b*}, Catherine Coates^a, Silke Kerruth^a, Urwa Arif^a, Christian Schulze^b, J. Simon Wiegert^{b2}, Michael Geeves^c, Thomas G. Oertner^b and Katalin Török^{a3}

^aMolecular and Clinical Sciences Research Institute, St George's, University of London, London SW17 0RE, UK; ^bInstitute for Synaptic Physiology, Center for Molecular Neurobiology Hamburg, Hamburg 20251, Germany; ^cSchool of Biosciences, University of Kent, Canterbury CT2 7NZ, UK

*These authors contributed equally to this work.

¹Current address: Department of Cellular and Molecular Physiology, Institute of Translational Medicine, University of Liverpool, Crown Street, Liverpool L69 3BX.

²Current address Research Group Synaptic Wiring and Information Processing, Center for Molecular Neurobiology Hamburg, 20251 Hamburg, Germany.

³To whom correspondence should be addressed: Dr Katalin Török, Molecular and Clinical Sciences Research Institute, St George's, University of London, London SW17 0RE, UK, Telephone: +442087255832; E-mail: ktorok@sgul.ac.uk

SI Methods

Materials. pRSET FLIPE-600n and pCMV(MinDis).iGluSnFR plasmids were a gift from Loren Looger (HHMI Janelia Research Campus, Ashburn, VA 20147) (Addgene Plasmid #41732) and Wolf Frommer (Heinrich Heine University, 40225 Düsseldorf, Germany) (Addgene plasmid # 13537), respectively. pET41a and pET30b vectors were obtained from Novagen. *E. coli* XL10-Gold and BL21 (DE3) Gold cells were purchased from Invitrogen. Restriction enzymes were obtained from New England Biolabs and T4 DNA ligase from Fermentas.

Cloning of glutamate binding proteins into bacterial expression vectors. The *iGluSnFR* gene was subcloned from pCMV(MinDis).iGluSnFR by restriction-ligation into pET41a (GST-fusion expression vector) at BglII and NotI restriction sites and *ybeJ* encoding GluBP was subcloned from pRSET FLIPE 600n (ECFP-*ybeJ*-Venus) into pET30b (His-fusion expression vector) at BglII and NotI restriction sites.

Site-directed mutagenesis of iGluSnFR. A series of DNA mutations were performed on pET41a-iGluSnFR. Site-directed mutagenesis was carried out following the QuikChange II XL protocol (Agilent Technologies) using the following primers (5'→3'):

R24K, GGTGTGATTGTCGTCGGTCACAAGGAATCTTCAGTGCCTTTCTCT;

E25A, GTCGTCGGTCACCGTGCATCTTCAGTGCCTTTC;

E25D, GATTGTCGTCGGTCACCGTGATTCTTCAGTGCC;

E25R, GATTGTCGTCGGTCACCGTAGATCTTCAGTGCCTTTCTCT;

S72T, GTAAACTGATTCCGATTACCACGCAAACCGTATTCCACTGCTG;

T92A, TTGAATGTGGTTCTACCGCCAACAACGTCGAACGC;

Mutations were confirmed by DNA sequencing (Genewiz).

Expression and purification of genetically encoded glutamate indicator (GEGI) proteins.

His-tagged GluBP, GST-fused iGluSnFR and variant proteins were overexpressed in *E. coli* BL21 (DE3) Gold cells. Cells were grown at 37 °C and expression was induced overnight at 20 °C in the presence of 0.5 mM isopropyl thio-β-D-galactoside (IPTG). Cells were resuspended in 50 mM Na⁺-HEPES, 200 mM NaCl, pH 7.5 containing one tablet of Complete protease inhibitor cocktail (Roche, Basel, Switzerland) and lysed by sonication on ice (VibraCell, Jencons PLS). For GST-fused proteins, clarified lysates were purified by a single-step GST chromatography (GSTrap, ÄKTA Purifier, GE Healthcare) at 4 °C. The purified protein was eluted in 50 mM Na⁺-HEPES, 200 mM NaCl, 10 mM reduced glutathione, pH 7.5. For His-tagged GluBP clarified lysate was purified on a NiNTA column (QIAGEN, ÄKTA Purifier, GE Healthcare) at 4 °C. The purified protein was eluted with a linear gradient of 0-0.5 M imidazole. Purity was assessed by SDS-PAGE (gradient of 6.4% - 20% acrylamide/bisacrylamide) and aliquoted fractions were dialyzed against 50 mM Na⁺-HEPES, 200 mM NaCl, pH 7.5 and stored at -80 °C.

Measuring protein concentrations. iGluSnFR and GluBP proteins were highly purified, allowing protein concentration to be determined spectroscopically. The absorption spectra of all iGluSnFR proteins comprised three peaks at wavelengths 280 nm, 400 nm and 497 nm. Protein concentrations were determined with molar extinction coefficients (ϵ_0) at 280 nm calculated from the amino acid composition using a Nanodrop 1000 spectrophotometer (Thermo Scientific). $\epsilon_{0(280)}$ of 90690 M⁻¹cm⁻¹ for GST-iGluSnFR and 24075 M⁻¹cm⁻¹ for His-GluBP was calculated (Gill and von Hippel, 1989).

Equilibrium binding titrations for iGluSnFR proteins. Glutamate affinity assays of iGluSnFR proteins were performed by continuous titration using an automated syringe pump (ALADDIN 1000, WPI). iGluSnFR and variants at 50-100 nM concentration (50 mM Na⁺-HEPES, 100 mM NaCl, 2 mM MgCl₂, pH 7.5 at 20 °C) were titrated with an appropriate stock solution of glutamate at a 10 μL/min flow rate in a stirred 3 mL cuvette. Fluorescence was measured at 492 nm excitation and 512 nm emission wavelengths using a Fluorolog3 spectrofluorimeter (Horiba Scientific). Fluorescence records were corrected for dilution and photobleaching (0.1%/min). Data were normalized and expressed as bound fraction and glutamate dissociation constant (K_d) and cooperativity (n) were obtained by fitting the data to the Hill equation using GraphPad Prism 7 software. All titrations were performed at least in triplicates and expressed as mean ± SEM. Ligand binding specificity was assessed by titrating iGluSnFR proteins as described above with L-aspartate, L-glutamine, D-serine, GABA and glycine.

Stopped-flow fluorimetry. Glutamate association and dissociation kinetic experiments of iGluSnFR proteins were carried out on a Hi-Tech Scientific SF-61DX2 stopped-flow system equipped with a temperature manifold (Walklate and Geeves, 2015) in the 4 °C to 34 °C temperature range, as specified. Fluorescence excitation was set to 492 nm. Fluorescence emission was collected using a 530 nm cut-off filter. At least 3 shots from 3 replicates were averaged for analysis. Data were fitted to a single exponential to obtain the fluorescence rise or decay rate using KinetAssyst software (TgK scientific).

Association kinetics. The solution containing 1 μM protein in 50 mM Na⁺-HEPES, 100 mM NaCl, 2 mM MgCl₂, pH 7.5 was rapidly mixed (1:1) with 50 mM Na⁺-HEPES, 100 mM NaCl, 2 mM MgCl₂, pH 7.5 containing increasing glutamate concentrations (concentrations given are those in the mixing chamber). For the determination of temperature dependence of glutamate association rates, protein samples at 1 μM concentration were mixed as above to give a final glutamate concentration of 1 mM for iGluSnFR, 5 mM for iGluSnFR E25D (iGlu_f) and 10 mM for iGluSnFR S72T (iGlu_u) in the mixing chamber.

Dissociation kinetics. The solution containing 1 μM protein in 50 mM Na⁺-HEPES, 100 mM NaCl, 2 mM MgCl₂, pH 7.5 with saturating glutamate (15 x K_d) was rapidly mixed (1:1) with 0.67 mM GluBP in 50 mM Na⁺-HEPES, 100 mM NaCl, 2 mM MgCl₂, pH 7.5 (concentrations in the mixing chamber). For the determination of temperature dependence of glutamate dissociation rates, protein samples at 1 μM concentration were premixed to give a final glutamate concentration of 0.2 mM for iGluSnFR, 0.5 mM for iGlu_f and 1 mM for iGlu_u in the mixing chamber.

pH sensitivity of iGluSnFR, iGlu_f and iGlu_u proteins. To determine the apparent pK_a for iGluSnFR proteins, a series of buffers were prepared. Depending on their respective pH buffering range, appropriate buffer was used for the measurements (MES for pH 6 - 6.5, HEPES for pH 7 - 8, Tris for pH 8.5 - 9 and CAPS for pH 10). The pH titrations were performed by recording fluorescence spectra in glutamate-free (50 mM Na⁺-buffer, 100 mM NaCl, 2 mM MgCl₂) or glutamate-saturated (50 mM Na⁺-buffer, 100 mM NaCl, 2 mM MgCl₂, 1 - 10 mM glutamate) using 1 μM protein in 0.5 pH unit intervals (Fluorolog3, Horiba). Final glutamate concentrations were 1 mM for iGluSnFR, 2 mM for iGlu_f and 10 mM for iGlu_u.

Quantum yield determination. The concentration of iGluSnFR proteins was adjusted such that the absorbance at the excitation wavelength (492 nm) was between 0.001 and 0.04. A

series of dilutions was prepared in a buffered solution (50 mM Na⁺-HEPES, 100 mM NaCl, 2 mM MgCl₂, pH 7.5 with either no glutamate or 1 - 10 mM glutamate. Final glutamate concentrations were 1 mM for iGluSnFR, 2 mM for iGlu_f and 10 mM for iGlu_u. Fluorescence spectra were recorded on a Fluorolog3 (Horiba Scientific). GCaMP6f quantum yield measured in Ca²⁺-saturated buffer was used as a reference ($\Phi_{+Ca^{2+}} = 0.59$) (Chen et al., 2013). Data were plotted as integrated fluorescence intensity as a function of absorbance and fitted to a linear regression with slope S. Quantum yield for iGluSnFR proteins was obtained using the following equation: $\Phi_{\text{protein}} = \Phi_{\text{GCaMP6f}} \times (S_{\text{protein}}/S_{\text{GCaMP6f}})$.

***In situ* glutamate titration.** HEK293T cells were cultured on 24-well glass bottom plates in DMEM containing non-essential amino-acids (Life Technologies), 10% heat inactivated FBS (Life Technologies) and penicillin/streptomycin (100 U/ml, 100 mg/ml, respectively), at 37 °C in an atmosphere of 5% CO₂. Cells were allowed 24 h to adhere before transfection with Lipofectamine 2000 (Invitrogen) following the manufacturer's recommendations (1.5 μL Lipofectamine 2000 and 0.5 μg plasmid DNA in 50 μL OptiMEM (Life Technologies)) and maintained for 24 h before being used in experiments. HEK293T cells transfected with iGluSnFR, iGlu_f or iGlu_u were washed with PBS and imaged in 20 mM Na⁺-HEPES, 145 mM NaCl, 10 mM glucose, 5 mM KCl, 1 mM MgCl₂, 1 mM NaH₂PO₄, pH 7.4. Cells were examined at 37 °C (OKO lab incubation chamber) with a 3i Marianas spinning-disk confocal microscope equipped with a Zeiss AxioObserver Z1, a 40x/NA1.3 oil immersion objective and a 3i Laserstack as excitation light source (488 nm). Emitted light was collected through a 525/30 nm BrightLine[®] single-band bandpass filter (Yokogawa CSU-X filter wheel) onto a CMOS camera (Hamamatsu, ORCA Flash 4.0; 1152x1656 pixels). Glutamate titrations were carried out using 0 - 10 mM L-glutamate (final concentration). Regions of interest (ROI) were defined by ellipses along each cell membrane. A single ROI was analyzed in each cell. ImageJ was used to process the images. GraphPad Prism 7 was used to plot and fit data with the Hill equation. The number of cells analyzed (n) were between 19 and 41, as specified. Data was expressed as mean ± SEM.

Organotypic slice cultures and single cell electroporation. Organotypic hippocampal slices were prepared from male Wistar rats at post-natal day 5 as described (Gee et al., 2017). Briefly, dissected hippocampi were cut into 400 μm slices with a tissue chopper and placed on a porous membrane (Millicell CM, Millipore). Cultures were maintained at 37 °C, 5% CO₂ in a medium containing 80% MEM (Sigma M7278), 20% heat-inactivated horse serum (Sigma H1138) supplemented with 1 mM L-glutamine, 0.00125% ascorbic acid, 0.01 mg/ml insulin, 1.44 mM CaCl₂, 2 mM MgSO₄ and 13 mM D-glucose. No antibiotics were added to the culture medium. DNA encoding iGluSnFR and tdimer2 were subcloned into a mammalian expression vector (pCI) under the control of the neuron-specific human synapsin1 promoter. iGlu_f and iGlu_u were generated by site-directed mutagenesis of pCI-synapsin-iGluSnFR using the oligonucleotides for the E25D (iGlu_f) and S72T (iGlu_u) mutations. Individual CA3 pyramidal cells were transfected by single-cell electroporation (Wiegert et al., 2017a; Wiegert et al., 2017b). iGluSnFR and variant plasmids were electroporated at 40 ng/μL (iGluSnFR) or 50 ng/μL (iGlu_f, iGlu_u) along with a cytoplasmic red fluorescent protein tdimer2 (20 ng/μL). During electroporation slices were kept in 10 mM Na⁺-HEPES, 145 mM NaCl, 25 mM D-glucose, 1 mM MgCl₂ and 2 mM CaCl₂, pH 7.4.

Electrophysiology. Experiments were performed between 14-30 days *in vitro* (2 - 4 days after electroporation). Hippocampal slice cultures were placed in the recording chamber of the microscope and superfused with artificial cerebrospinal fluid (ACSF) containing 25 mM NaHCO₃, 1.25 mM NaH₂PO₄, 127 mM NaCl, 25 mM D-glucose, 2.5 mM KCl and (saturated

with 95% O₂ - 5% CO₂), 2 mM CaCl₂ and 1 mM MgCl₂. Whole-cell patch clamp recordings from a transfected CA3 pyramidal neurons were performed with a Multiclamp 700B amplifier (Molecular Devices) under the control of Ephus software written in MATLAB (Suter et al., 2010). CA3 neurons were held in current clamp and stimulated through the patch pipette by brief electrical pulses (2 - 3 ms and 1500 - 3500 pA current injection) to induce single action potentials. Analog signals were filtered at 6 kHz and digitized at 10 kHz. Patch pipettes with a tip resistance of 3.5 to 4.5 MΩ were pulled with a Narishige PC-10 vertical puller and filled with 10 mM K⁺-HEPES, 135 mM K⁺-gluconate, 4 mM MgCl₂, 4 mM Na⁺₂-ATP, 0.4 mM Na⁺-GTP, 10 mM Na⁺₂-phosphocreatine and 3 mM ascorbate (pH 7.2). Slice experiments were performed at 34 ± 1 °C by controlling the temperature of the ACSF with an in-line heating system and the oil immersion condenser with a Peltier element. Dual patch experiments and iGlu_u measurements (**Fig. 3**) were done under NMDAR block (10 μM CPP-ene) to prevent induction of long-term plasticity during high frequency stimulation.

Two-photon microscopy and data analysis. The custom-built two-photon imaging setup was based on an Olympus BX51WI microscope controlled by a customized version the open-source software package ScanImage (Pologruto et al., 2003) written in MATLAB (MathWorks). We used a pulsed Ti:Sapphire laser (MaiTai DeepSee, Spectra Physics) tuned to 980 nm wavelength to simultaneously excite both the cytoplasmic tdimer2 and the membrane bound iGluSnFR. Red and green fluorescence was detected through the objective (LUMPLFLN 60XW, 60x, NA 1.0, Olympus) and through the oil immersion condenser (NA 1.4, Olympus) using 2 pairs of photomultiplier tubes (PMTs, H7422P-40SEL, Hamamatsu). 560 DXCR dichroic mirrors and 525/50 and 607/70 emission filters (Chroma Technology) were used to separate green and red fluorescence. Excitation light was blocked by short-pass filters (ET700SP-2P, Chroma). ScanImage was modified for the user to freely define the scanning path. Signals from iGluSnFR and fast variants were measured by repeatedly scanning a spiral line across the bouton to maximize the signal-to-noise ratio. iGluSnFR signals were sampled at 500 Hz and iGlu_f and iGlu_u signals were sampled either at 500 Hz or 1 kHz.

Fluorescence was monitored at single Schaffer collateral terminals in CA1 while action potentials were triggered by brief (2 ms) depolarizing current injections into the soma of the transfected CA3 neuron. As the precise orientation of the synaptic cleft on the bouton was unknown to us, we used rapid spiral scans to sample the entire surface of the bouton. A spiral scan covering the entire bouton may hit the diffusing cloud of glutamate just once or several times per line. Typically, the spiral scan line intersected the release site multiple times (**Fig. 1 j,k**). To maximize the signal-to-noise ratio in every trial, we assigned a dynamic region of interest (ROI): pixel columns (i.e. spatial positions) were sorted according to the change in fluorescence (ΔF) in each column (**Fig. 1 j, SI Appendix Fig. S2**). To analyze individual trials, we sorted the columns (corresponding to positions along the scan line) according to their relative increase in fluorescence ($\Delta F/F_0$) and evaluated the top 50% for iGluSnFR signals and the top 63.2% for iGlu_u and iGlu_f signals (ROI). In contrast to straight line scans, this method was robust against small movements of the bouton between trials (tissue drift). While 500 Hz sampling was sufficient for iGluSnFR, we increased the scanning speed to 1 kHz to capture the peak of the very brief iGlu_u response (**Fig. 1 k**). The peak amplitudes were extracted from the average of 10 trials acquired at 0.1 Hz (**Fig. 3 a**). To avoid bleach-related run-down during the train, we normalized each of the 11 peaks by a baseline measurement (F_0) taken just 1 ms before. This strategy was possible since the inter-stimulus interval was 10 ms (500 ms for pulse #11) and τ_{off} was 2.6 ms.

For the peak amplitude measurement of postsynaptic AMPA responses (**Fig. 3 a**), we repeated the protocol 70 - 100 times at 0.1 Hz and manually removed trials in which the CA1 neuron received spontaneous synaptic input. In addition, we discarded trials where the patch-

clamped CA3 neuron failed to spike in response to a somatic current injection, and averaged the remaining trials. The decay time course of the recovery action potential was fitted with a mono-exponential decay function. This decay time constant was then used to extract the amplitude of individual responses during the 100 Hz train by deconvolution. Analysis was done in MATLAB and GraphPad Prism.

Data analysis and kinetic modelling. Biophysical experiments were performed at least in triplicates and analysed using GraphPad Prism 7 and KinetAsyst (TgK Scientific) software. Experiments on HEK293T cells were carried out on three independent cultures each. The total number of cells analysed in each condition is given in the figure legends. The software package IBS (<http://ibs.biocuckoo.org>) was used to display the domain structure glutamate sensors. The PyMOL Molecular Graphics System (2002) by W. L. Delano (<https://www.pymol.org/> RRID: SCR_000305) was employed for displaying the crystal structure. Global fitting to kinetic data was performed using DynaFit4 software (<http://www.biokin.com/dynafit> RRID: SCR_008444) according to the **Schemes 1 & 2**.

Kinetic theory. iGluSnFR is represented as iGlu_l~iGlu_s, indicating that the N-terminally flanking large GluBP fragment (GluBP 1-253, iGlu_l) and the C-terminally fused small GluBP fragment (GluBP 254-279, iGlu_s) are within one molecule but separated by the interjecting cpEGFP.

Scheme 1:



Glutamate binds to the large domain iGlu_l of GluBP. This is a pre-equilibrium that is described by the following equation:

$$\frac{\partial [Glu \cdot iGlu_l \sim iGlu_s]}{\partial t} = k_{+1} [iGlu_l \sim iGlu_s] [Glu] - k_{-1} [Glu \cdot iGlu_l \sim iGlu_s] \quad (1)$$

With the equilibrium constant defined as:

$$K_1 = \frac{k_{+1}}{k_{-1}} \quad (2)$$

The total concentration of iGluSnFR, $[iGluSnFR]_0$ is the sum of all iGluSnFR complexes involved in the scheme.

$$[iGluSnFR]_0 = [iGlu_l \sim iGlu_s] + [Glu \cdot iGlu_l \sim iGlu_s] + [Glu \cdot iGlu_c^*] \quad (3)$$

From this term $[iGlu_l \sim iGlu_s]$ is derived as:

$$[iGlu_l \sim iGlu_s] = [iGluSnFR]_0 - [Glu \cdot iGlu_l \sim iGlu_s] - [Glu \cdot iGlu_c^*] \quad (4)$$

If steady-state is assumed for the glutamate-bound iGluSnFR ($Glu \cdot iGlu_l \sim iGlu_s$) then **eq. 1** equals zero and we can insert **eq. 4** to obtain a term for $[Glu \cdot iGlu_l \sim iGlu_s]$.

$$[Glu \cdot iGlu_l \sim iGlu_s] = \frac{K_1 [Glu]}{1 + K_1} \cdot ([iGluSnFR]_0 - [Glu \cdot iGlu_c^*]) \quad (5)$$

The formation of the fluorescent state $[Glu \cdot iGlu_c^*]$ is defined by:

$$\frac{\partial [Glu \cdot iGlu_c^*]}{\partial t} = k_{+2} [Glu \cdot iGlu_l \sim iGlu_s] - k_{-2} [Glu \cdot iGlu_c^*] \quad (6)$$

Inserting **eq. 5** into **eq. 6** and performing a partial differentiation leads to:

$$k_{obs} = \frac{k_{+2}K_1[Glu]}{1+K_1[Glu]} + k_{-2} \quad (7)$$

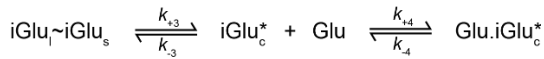
With the amplitude A , the $K_{overall}$ and K_d defined as:

$$A = \frac{k_{+2}K_1[Glu][iGluSnFR]_0}{1+K_1[Glu]}$$

$$K_{overall} = K_1(1 + K_2)$$

$$K_d = \frac{1}{K_o} = \frac{1}{K_1+K_1K_2} \quad (8a,b,c)$$

Scheme 2:



$iGlu_l \sim iGlu_s$ first forms the complete state $iGlu_c^*$ that is fluorescent. The pre-equilibrium can be defined as:

$$\frac{\partial [iGlu_c^*]}{\partial t} = k_{+3}[iGlu_l \sim iGlu_s] - k_{-3}[iGlu_c^*] \quad (9)$$

With the equilibrium constant defined as:

$$K_3 = \frac{k_{+3}}{k_{-3}} \quad (10)$$

The total concentration of $iGluSnFR$, $[iGluSnFR]_0$ is the sum of all $iGluSnFR$ complexes involved in the scheme.

$$[iGluSnFR]_0 = [iGlu_l \sim iGlu_s] + [iGlu_c^*] + [Glu \cdot iGlu_c^*] \quad (11)$$

From this term $[iGlu_l \sim iGlu_s]$ is derived as:

$$[iGlu_l \sim iGlu_s] = [iGluSnFR]_0 - [iGlu_c^*] - [Glu \cdot iGlu_c^*] \quad (12)$$

If steady-state is assumed for ($iGlu_c^*$) then **eq. 9** equals zero and we can insert **eq. 12** to obtain a term for $[iGlu_c^*]$.

$$[iGlu_c^*] = \frac{K_3}{1+K_3} \cdot ([iGluSnFR]_0 - [Glu \cdot iGlu_c^*]) \quad (13)$$

The formation of the fluorescent state $[Glu \cdot iGlu_c^*]$ is defined by:

$$\frac{\partial [Glu \cdot iGlu_c^*]}{\partial t} = k_{+4}[iGlu_c^*][Glu] - k_{-4}[Glu \cdot iGlu_c^*] \quad (14)$$

Inserting **eq. 13** into **eq. 14** and performing a partial differentiation leads to:

$$k_{obs} = \frac{k_{+4}K_3[Glu]}{1+K_3} + k_{-4} \quad (15)$$

With the amplitude A , the $K_{overall}$ and K_d defined as:

$$A = \frac{k_{+4}K_3[Glu][iGluSnFR]_0}{1 + K_3}$$

$$K_{overall} = K_3(1 + K_4)$$

$$K_d = \frac{1}{K_o} = \frac{1}{K_3 + K_3 K_4}$$

(16a,b,c)

Reference List

- Chen TW, Wardill TJ, Sun Y, Pulver SR, Renninger SL, Baohan A, Schreiter ER, Kerr RA, Orger MB, Jayaraman V, Looger LL, Svoboda K, Kim DS (2013) Ultrasensitive fluorescent proteins for imaging neuronal activity. *Nature* 499:295-300.
- Gee CE, Ohmert I, Wiegert JS, Oertner TG (2017) Preparation of Slice Cultures from Rodent Hippocampus. *Cold Spring Harb Protoc* 2017:db.
- Gill SC, von Hippel PH (1989) Calculation of protein extinction coefficients from amino acid sequence data. *Anal Biochem* 182:319-326.
- Pologruto TA, Sabatini BL, Svoboda K (2003) ScanImage: flexible software for operating laser scanning microscopes. *Biomed Eng Online* 2:13.
- Suter BA, O'Connor T, Iyer V, Petreanu LT, Hooks BM, Kiritani T, Svoboda K, Shepherd GM (2010) Ephus: multipurpose data acquisition software for neuroscience experiments. *Front Neural Circuits* 4:100.
- Walklate J, Geeves MA (2015) Temperature manifold for a stopped-flow machine to allow measurements from -10 to +40 degrees C. *Anal Biochem* 476:11-16.
- Wiegert JS, Gee CE, Oertner TG (2017a) Single-Cell Electroporation of Neurons. *Cold Spring Harb Protoc* 2017:db.
- Wiegert JS, Gee CE, Oertner TG (2017b) Viral Vector-Based Transduction of Slice Cultures. *Cold Spring Harb Protoc* 2017:db.

Figure S1

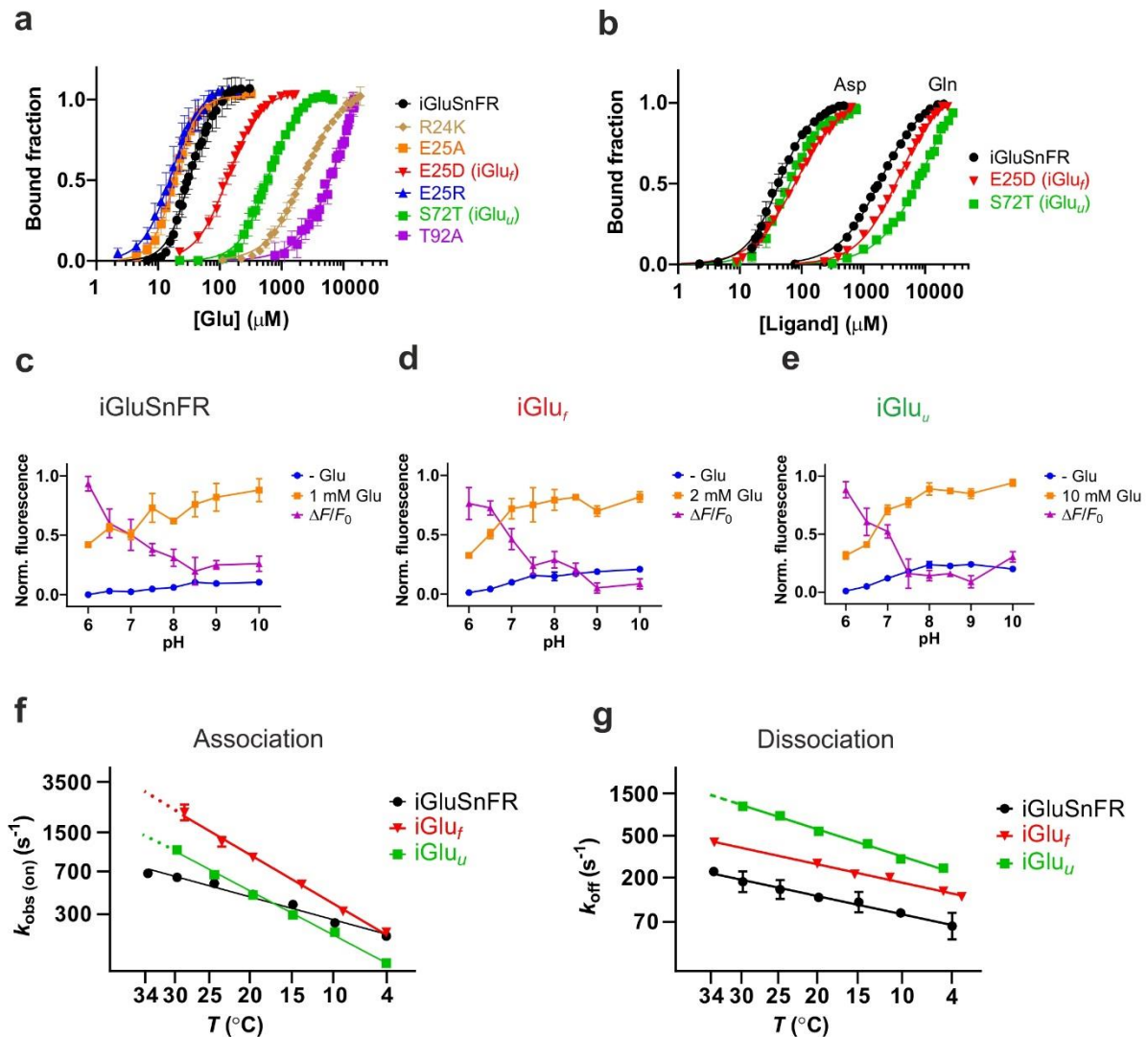


Fig. S1. Biophysical characterization of iGluSnFR variants. (a) Equilibrium glutamate binding titrations at 20 °C for iGluSnFR (●), iGluSnFR E25D (iGlu_f) (▼), iGluSnFR S72T (iGlu_u) (■), iGluSnFR E25R (▲), iGluSnFR E25A (■), iGluSnFR R24K (◆), iGluSnFR T92A (■). Fluorescence changes are normalized to F_0 of 0 and F_{max} of 1. (b) Ligand selectivity. Equilibrium titration of iGluSnFR (●), iGlu_f (▼) and iGlu_u (■) with aspartate and glutamine, as indicated. pH sensitivity and pK_a determination of (c) iGluSnFR; (d) iGlu_f; (e) iGlu_u. Normalized fluorescence in the presence of glutamate (■) (concentration as specified), or in the absence of glutamate (●); $\Delta F/F_0$ (▲). (f) Arrhenius plots of the limiting on-rates of iGluSnFR, iGlu_f and iGlu_u. Values at 34 °C for iGlu_f and iGlu_u are extrapolated assuming the measured slope. (g) Arrhenius plot of the dissociation rate constants of iGluSnFR, iGlu_f and iGlu_u. The value for iGlu_u 34 °C is extrapolated assuming the measured slope.

Figure S2

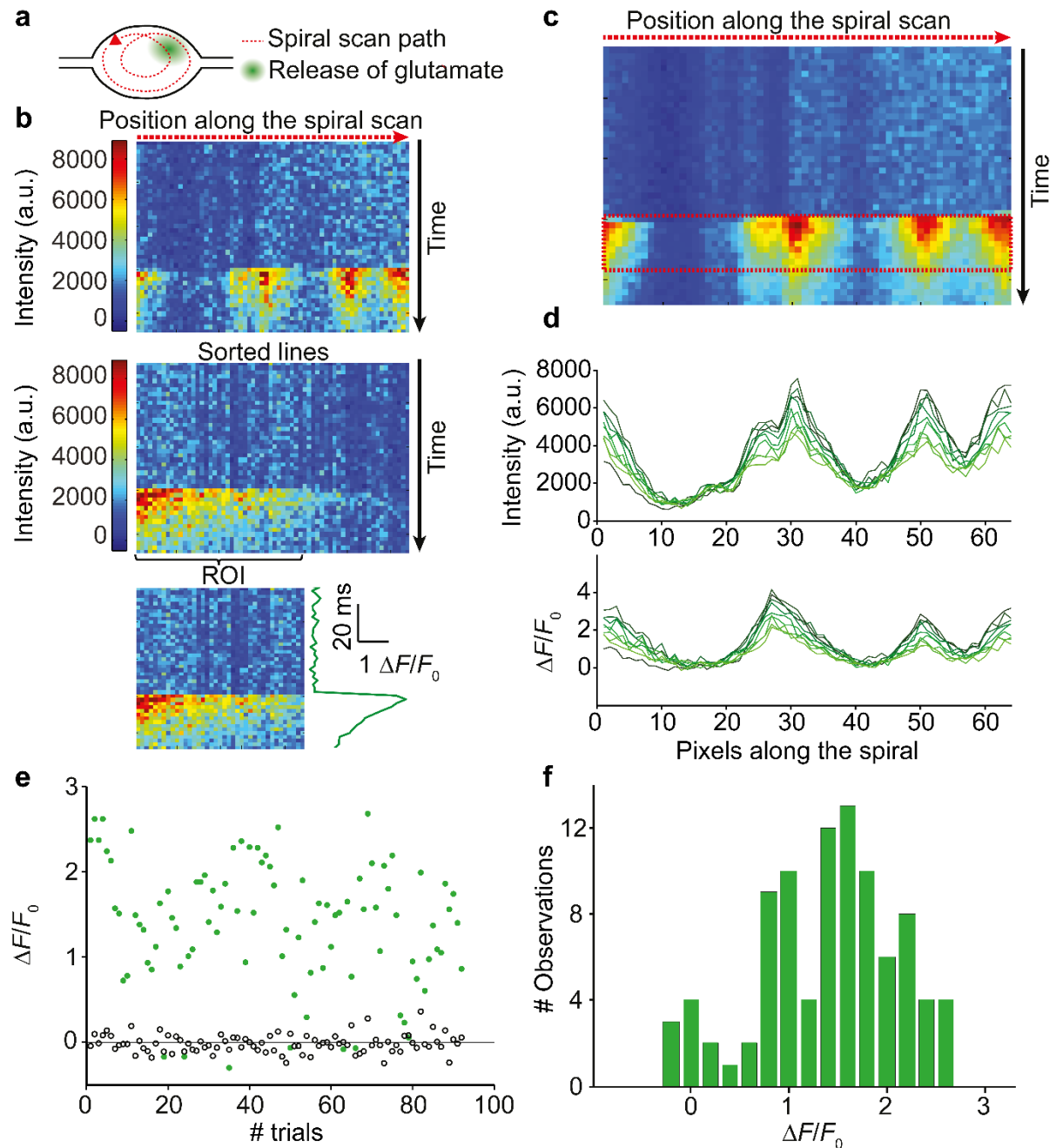


Fig. S2. Extraction of amplitudes from spiral scans of iGluSnFR signals. **(a)** Spiral scan intersecting the site of vesicular fusion. **(b)** Spiral scan, single trial response. Columns were sorted according to the signal amplitude (ΔF). The region of interest (ROI) was defined as the columns with $\Delta F > 50\%$ of maximum ΔF (63.2% of maximum for iGlu_{ii}). **(c)** Average of 10 trials (single APs) to analyze lateral spread of signal (red box). **(d)** Decay of fluorescence transient (9 scan lines = 18 ms). Note lack of lateral spread of the signal due to slow diffusion of membrane-anchored iGluSnFR. **(e)** iGluSnFR responses from a single Schaffer collateral bouton plotted over time. Single action potential stimulation, (●); No stimulation, (○). Note clear separation of successes and failures. **(f)** Histogram of response amplitudes displayed in panel (e); multiple peaks may be due to multi-vesicular release events.

Figure S3

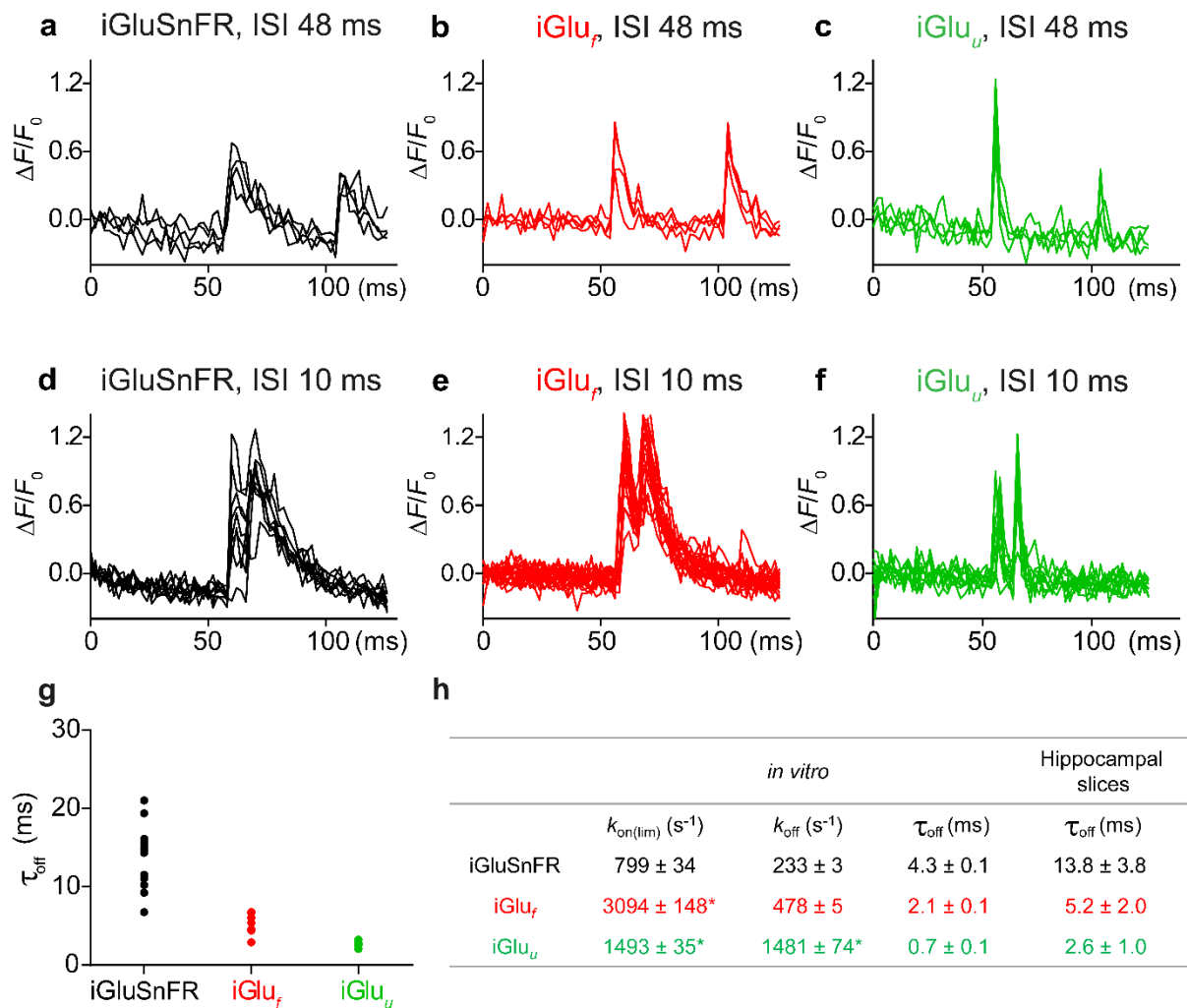


Fig. S3. Fluorescence time course ($\Delta F/F_0$) in single boutons expressing (a) iGluSnFR, (b) $iGlu_f$ or (c) $iGlu_u$ stimulated by a somatic paired pulse (48 ms ISI). Fluorescence time course ($\Delta F/F_0$) of single boutons expressing (d) iGluSnFR, (e) $iGlu_f$ or (f) $iGlu_u$ stimulated by a somatic paired pulse (10 ms ISI). (g) Decay time constant τ_{off} measured in hippocampal slices at 34 °C for iGluSnFR (n = 13, 500 Hz sampling rate), $iGlu_f$ (n = 7, 1 kHz sampling rate) and $iGlu_u$ (n = 7, 1 kHz sampling rate). (h) Summary of *on*- and *off*-rates *in vitro* and decay times measured *in vitro* and in hippocampal slices at 34 °C. Values are given as mean \pm SEM. Values marked by * are extrapolated from Arrhenius plots (Fig. S1 f,g).

Figure S4

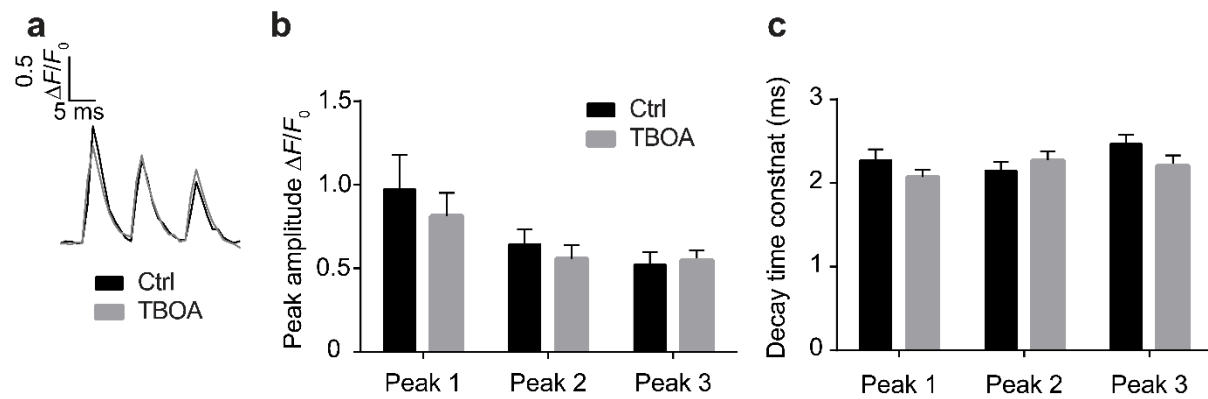


Fig. S4. Testing the effect of glutamate uptake blocker DL-threo- β -Benzyloxyaspartate (DL-TBOA) on synaptic $iGlu_u$ transients. **(a)** Average traces ($iGlu_u$) from single Schaffer collateral boutons stimulated at 100 Hz, before and after wash-in of TBOA (40 μ M). **(b)** Peak amplitude was not affected by TBOA ($n = 10$ boutons) **(c)** Decay kinetics was not affected by TBOA ($n = 10$ experiments).

Figure S5

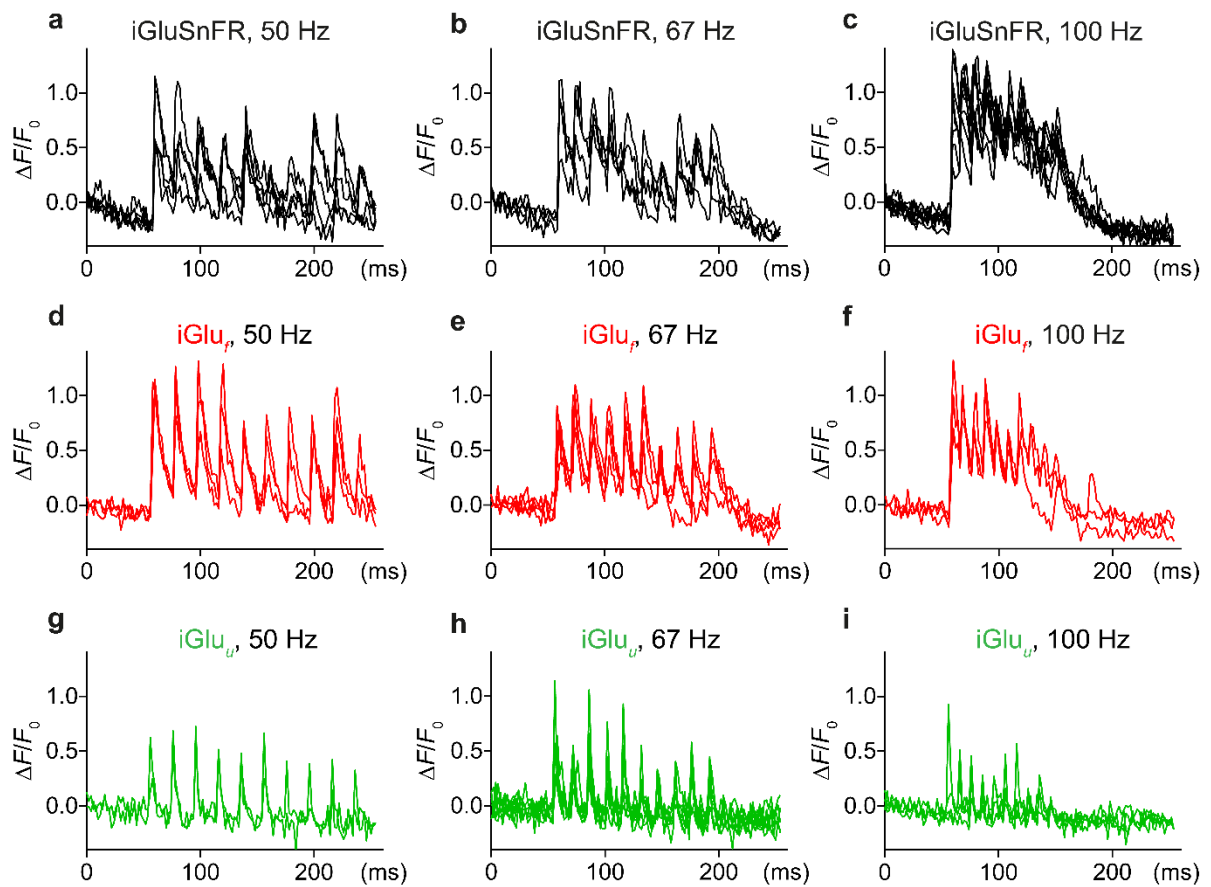


Fig. S5. Fluorescence time course ($\Delta F/F_0$) in single boutons expressing (a-c) iGluSnFR, (d-f) iGlu_f and (g-i) iGlu_u stimulated by 10 APs fired at (a, d, g) 50 Hz, (b, e, h) 67 Hz and (c, f, i) 100 Hz. Number of trials: (a), 5; (b), 4; (c), 8; (d), 3; (e), 4; (f), 3; (g), 2; (h), 7; (i), 4.

Figure S6

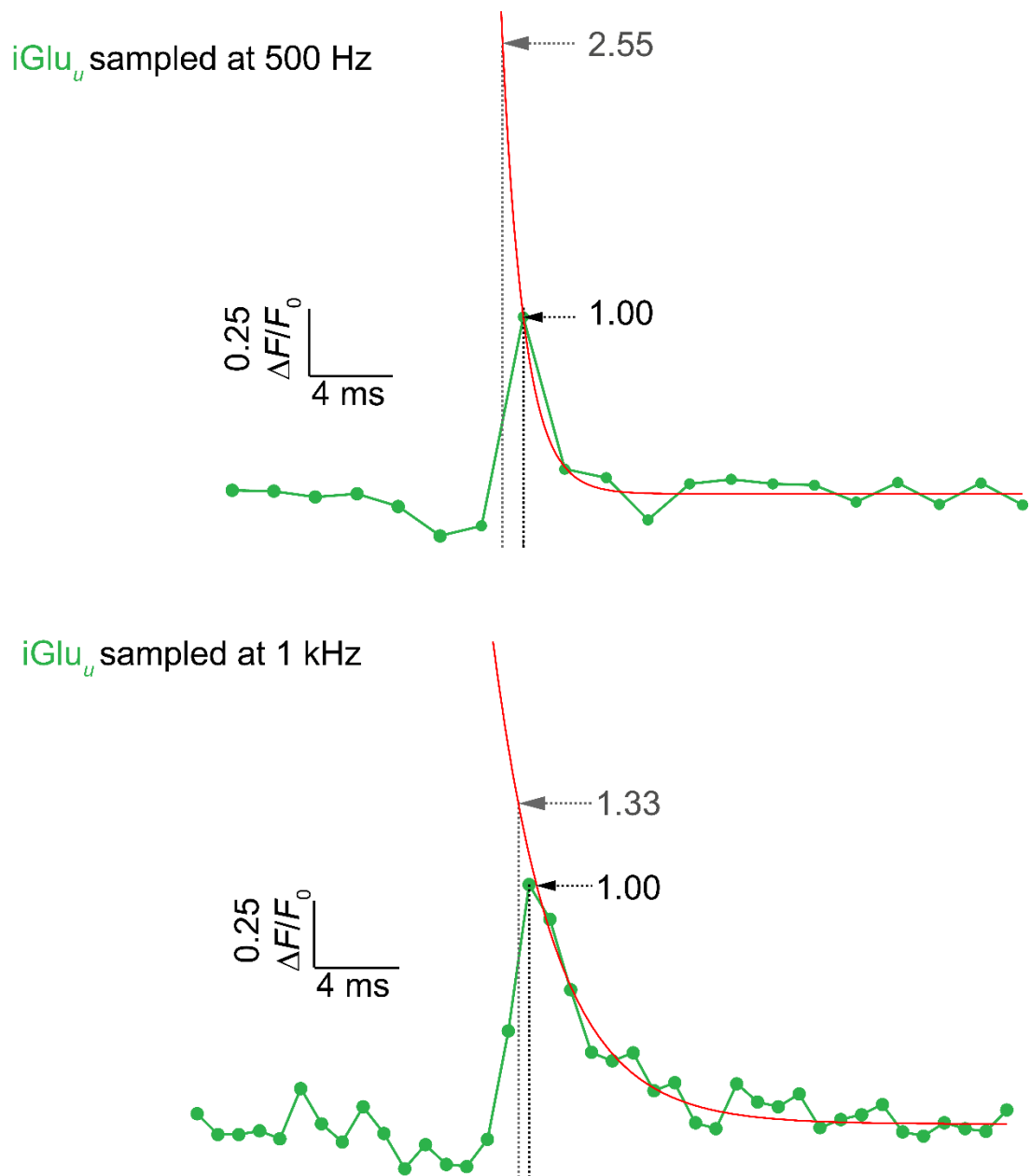


Fig. S6. Estimating peak amplitudes at different sampling frequencies. When sampling iGlu_u fluorescence at 500 Hz, it is possible to miss the peak of the fluorescence transient. Sampling at 1 kHz reduces the potential error to ~33%.

Table S1. Brightness of iGluSnFR variants.

Protein	Φ		$\epsilon_{o(492nm)}$ ($M^{-1} cm^{-1}$)		Brightness ($mM^{-1} cm^{-1}$)	
	-Glu	+Glu	-Glu	+Glu	-Glu	+Glu
iGluSnFR	0.65 ± 0.02	0.66 ± 0.02	9294 ± 86	38801 ± 293	6.1 ± 0.2	25.4 ± 0.8
iGlu _r	0.65 ± 0.02	0.68 ± 0.02	8789 ± 76	28644 ± 127	5.7 ± 0.2	19.4 ± 0.6
iGlu _u	0.67 ± 0.02	0.67 ± 0.02	7895 ± 105	22796 ± 120	5.3 ± 0.2	15.3 ± 0.5

Brightness values were obtained from quantum yield and ϵ_o measurements.

Table S2. Fluorescence and equilibrium glutamate binding properties of iGluSnFR variants.

Protein	F_r^a		$F_{r(+Glu)} / F_{r(-Glu)}$	K_d (μM)	n
	-Glu	+Glu			
iGluSnFR	1.0	5.4	5.4 ± 0.7	33 ± 1	2.3 ± 0.2
S72T (iGlu _u)	1.1	4.2	3.8 ± 0.6	600 ± 16	1.8 ± 0.1
E25D (iGlu _f)	1.8	7.2	4.0 ± 0.3	137 ± 4	1.7 ± 0.1
E25A	3.6	12.3	3.4 ± 0.6	18.6 ± 0.1	2.6 ± 0.1
E25R	4.7	7.3	1.6 ± 0.5	19.3 ± 0.8	2.3 ± 0.2
R24K	1.5	3.1	2.1 ± 0.1	$(2.3 \pm 0.1) \times 10^3$	1.5 ± 0.1
T92A	0.7	1.2	1.7 ± 0.5	$(12 \pm 4) \times 10^3$	1.3 ± 0.2

^aRelative fluorescence values were determined using apo-iGluSnFR as reference ($F_r = 1$).

Table S3. Selectivity of iGluSnFR, iGlu_f and iGlu_u for L-aspartate and L-glutamine.

Protein	$F_{(+Asp)} / F_{(-Asp)}$	$K_{d(Asp)}$ (μM)	n	$F_{(+Gln)} / F_{(-Gln)}$	$K_{d(Gln)}$ (μM)	n
iGluSnFR	4.7 ± 0.3	44.6 ± 0.3	1.6 ± 0.1	6.4 ± 0.8	1900 ± 100	1.3 ± 0.1
iGlu _f	2.7 ± 0.2	82.0 ± 0.6	1.2 ± 0.1	5.6 ± 0.5	3700 ± 100	1.3 ± 0.1
iGlu _u	1.6 ± 0.2	61.7 ± 0.4	1.7 ± 0.1	2.3 ± 0.3	10800 ± 300	1.1 ± 0.1

^aFluorescence dynamic range is reported as fold enhancement by aspartate or glutamine ligand binding.

Table S4. Kinetic properties of fast iGluSnFR variants **iGlu_r** and **iGlu_u**.

Protein	K_d (μM)	n	$k_{\text{on(lim)}}$ (s^{-1})	$t_{1/2(\text{on(lim)})}$ (ms)	k_{off} (s^{-1})	$t_{1/2(\text{off})}$ (ms)
iGluSnFR	33 ± 1	2.3 ± 0.2	643 ± 23	1.1 ± 0.1	110 ± 4	8.5 ± 0.4
E25D (iGlu_r)	137 ± 4	1.7 ± 0.1	1240 ± 77	0.6 ± 0.1	283 ± 36	2.4 ± 0.3
S72T (iGlu_u)	600 ± 16	1.8 ± 0.1	604 ± 12	1.1 ± 0.1	468 ± 58	1.5 ± 0.2

K_d and Hill coefficient (n) values were obtained from the equilibrium glutamate titrations at 20 °C. Fluorescence rise (limiting rate, $k_{\text{on(lim)}}$) and decay (k_{off}) rates were measured by glutamate association and dissociation stopped-flow kinetic experiments.

Table S5. Fitted and modelled kinetic parameters of the fluorescence response of iGluSnFR variants.

Scheme 1	K_1 (M^{-1})	K_2	$K_d(\text{calculated})$ (M)	k_{+1} ($M^{-1}s^{-1}$)	k_{-1} (s^{-1})	k_{+2} (s^{-1})	k_{-2} (s^{-1})	K_1k_{+2} ($M^{-1}s^{-1}$)	$K_d(\text{measured})$ (M)	n
iGluSnFR (20 °C)	3642	5.2	3.6×10^{-5}	2.7×10^7	5965	569	110	2.1×10^6	3.3×10^{-5}	2.3
iGluSnFR (34 °C)	3431	3.4	6.6×10^{-5}	2.8×10^7	8161	756	220	2.6×10^6	4.0×10^{-5}	1.7
Glu_f (20 °C)	1568	2.35	1.47×10^{-4}	3.5×10^6	2206	944	283	1.5×10^6	1.37×10^{-4}	1.7
iGlu_u (20 °C)	1291	0.29	6.00×10^{-4}	2.2×10^6	1704	136	468	1.7×10^5	6.00×10^{-4}	1.8

Fitted parameters to the kinetic model illustrated in **Fig. 4g** are shown for iGluSnFR and fast variants. Fitting the association kinetic records to **Scheme 1 (SI Methods, Kinetic Theory)** gives parameters for a hyperbole, K_1 , $k_{+2} + k_{-2}$, k_{-2} and the initial gradient, the apparent association rate constant K_1k_{+2} . Values for k_{+1} and k_{-1} were obtained by global fitting using Dynafit and represent a lower limit of values. The measured and calculated overall K_d values were in good agreement.